Graphene enhanced LiFeBO₃/C composites as cathodes for Li-ion batteries

Dongyun Zhang[1,*], Jin Qiao[1], Xiaoxiao Dong[1] Bingyan Xu[2], Runfa Li[1], Chengkang Chang[1,*]

[1] School of Materials Science and Engineering, Shanghai Institute of Technology,
[2] STATE GRID Shanghai Jinshan Electric Power Supply Company,
[*]E-mail: dyz@sit.edu.cn, ckchang@sit.edu.cn

Graphene enhanced LiFeBO₃/C composite electrodes are synthesized by a solid-state reaction. The effects of a graphene conductive additive on the LiFeBO₃/C electrodes are characterized by XRD, SEM and electrochemical tests. The results show that the electronic conductivities of the LiFeBO₃/C electrodes increase with increasing graphene content. The electronic conductivities of the LiFeBO₃/C electrodes with Super P (SP) and 5% graphene (5%GN+SP) are 5.16×10^{-3} S/cm and 1.65×10^{-2} S/cm, respectively. The lithium ion diffusion coefficient (D_{Li}) of the LiFeBO₃/C electrode with 3% graphene (3%GN+SP) is the highest at 9.85×10^{-14} cm² s⁻¹, which is much higher than that of the SP electrode (5.94×10^{-14} cm² s⁻¹). The 3%GN+SP electrode has the highest capacity of 189.6 mAh/g at 0.1 C, and its cyclic retention is 95% after 50 cycles at 1 C. The performance enhancement is mainly attributed to the moderate addition of the graphene conductor, which could improve both the electronic conductivity and ionic diffusion coefficient of the LiFeBO₃/C.

1. INTRODUCTION

During the past decades, olivine LiFePO₄ has dominated most of the electric vehicle power battery market, but its low theoretical capacity cannot satisfy the requirements for high-energy density products [1-3]. Due to the higher theoretical capacity (220 mAh/g), higher electronic conductivity (3.9×10^{-7}S/cm) and smaller volume change (2%) of LiFeBO₃, it has been considered a promising cathode alternative for lithium-ion batteries [4-9]. However, polyanion-type cathode materials have the common drawbacks of poor ionic and electronic conductivities. To overcome the above weaknesses, particle size reduction, ion doping, carbon coating and conductive additive addition have been used [6, 10-14]. Nano-sized mesoporous LiFeBO₃/C hollow spheres have been reported to deliver a high initial

reversible specific capacity of 190 mAh/g at 0.05 C [10]. Yamada and co-workers [12] reported that both of the discharge specific capacity and cycle performance of the $LiFeBO_3$ decreased after Mn doping, because the polarization of the electrodes becomes more severe with increasing Mn content. Nano-carbon web coated $LiFeBO_3$/C was synthesized by Zhang [6], which presented an initial discharge specific capacity of 196.5 mAh/g at 0.05 C.

In addition to directly modifying the $LiFeBO_3$ active materials, various sp2 carbon materials have been used as conductive additives in Li-ion batteries. Materials such as carbon black, conducting graphite, ethylene black, carbon nanotubes and graphene have proved to efficiently enhance the electronic conductivity of the $LiFePO_4$ cathode, and thus improving its electrochemical performance [15-20]. Super P has been used as a conventional conductor during the cathode preparation [11, 13]. However, graphene has many advantages over the conventional conductor Super P, such as high conductivity, sheet structure and small specific surface area. Trace amounts of graphene and Super P form an effective conducting network in which the positive active materials are embedded. Wu [18] reported that $LiFePO_4$ with graphene and Super P as conductive additives has better specific capacity and rate performance, which delivered an initial capacity of 165 mAh/g at 0.1 C, and even delivered a capacity of 112 mAh/g at the rate of 5 C. Gong [21] also improved the electrochemical performance of $LiFePO_4$ by combining different carbon materials. However, studies have rarely been performed to enhance the electrochemical performance of $LiFeBO_3$ by graphene conductive additives.

In this work, we prepared $LiFeBO_3$/C electrodes with different amounts of graphene conductive additives. The effects of graphene conductive additives on the electrochemical properties of the $LiFeBO_3$/C electrode were investigated. The results demonstrate that the performance of the $LiFeBO_3$/C electrode with part graphene conductive additives is much better than the system with single Super P additives, which is perfectly consistent with the above prediction.

2. EXPERIMENTAL

The $LiFeBO_3$/C samples were synthesized by a solid-state reaction. The raw materials were $LiOH \cdot H_2O$, $FeC_2O_4 \cdot 2H_2O$, H_3BO_3 and sucrose. First, the raw materials were mixed with deionized water and ball milled for 4 h. The rotation speed was 600 rpm, and the solid content was 20%. Second, the solution was dried to achieve the precursor by a spray dryer; the air pressure was 0.25 MPa; and the inlet and outlet air temperatures were 220°C and 120°C respectively. Finally, the as-prepared precursor was transfer to a tube furnace and calcined at 550°C for 7 h under an Ar atmosphere to obtain the $LiFeBO_3$/C composite.

CR2016 coin-type cells were assembled as follows. Super P (SP) purchased from Timcal. Ltd, Switzerland, and graphene (GN) purchased from Chengdu Organic Chemicals Co, Ltd. China were used as conductive additives. The positive electrodes were fabricated by blending the powders ($LiFeBO_3$/C) with the conductive additives and a polyvinylidene fluoride (PVDF) binder at a weight ratio of 8:1:1 in N-methyl-2-pyrrolidone (NMP). The resulting cathodes with SP, and SP and GN as the conductive additives were denoted as SP (LFB:SP:PVDF=80:10:10wt%), 1%GN+SP (LFB:SP:GN:PVDF=80:9.9:1:10wt%), 3%GN+SP (LFB:SP:GN:PVDF=80:9.7:3:10 wt%) and

5%GN+SP (LFB:SP:GN:PVDF=80:9.5:5:10wt%). Then, the electrodes were pressed into pellets of 12 mm in diameter containing 6 mg of active materials. Two-electrode electrochemical cells were assembled in a glove box filled with high-purity argon. The above mentioned $LiFeBO_3$ and lithium metal foil were used as the cathode and anode, respectively. Celgard2320 was used as separator. In addition, 1 M $LiPF_6$ in EC:DMC (1:1 vol.%) was used as the electrolyte. The electronic conductivity tests were performed on an RTS-4 linear four-point probe system. The prepared electrode paste was applied to the insulating layer to test the electronic conductivity. Then, the electronic conductivity was measured at five different positions on each of the $LiFeBO_3$/C pellets, which were 18 mm in diameter and 0.15 mm in thickness, to calculate the average electronic conductivity value.

X-ray powder diffraction (XRD, Bruker D8 Focus diffractometer) with Cu Kα radiation (0.1541 nm) was used to identify the phase at a scanning rate of 0.02°/s in the 2θ range from 10° to 70°. The sample morphology was monitored by a scanning electron microscope (SEM, JEOL, JSM-6700F), and elemental carbon analysis was performed by C S analysis equipment (Eltar, Germany).

Land Battery Testers (LAND-CT2001A) were used to test the electrochemical properties of the samples in the voltage range between 1.5 and 4.5 V. The cycle performance test was carried out at 1 C. The rate performance was monitored by charging and discharging at various rates ranging from 0.1 C to 5 C. The electrochemical impedance spectroscopy (EIS) measurements were conducted using an electrochemical workstation (Autolab PGSTAT302N) with a frequency range from 10^{-2} to 10^5 Hz at an amplitude of 5 mV. All the electrochemical measurements were carried out at room temperature (25°C).

3. RESULTS AND DISCUSSION
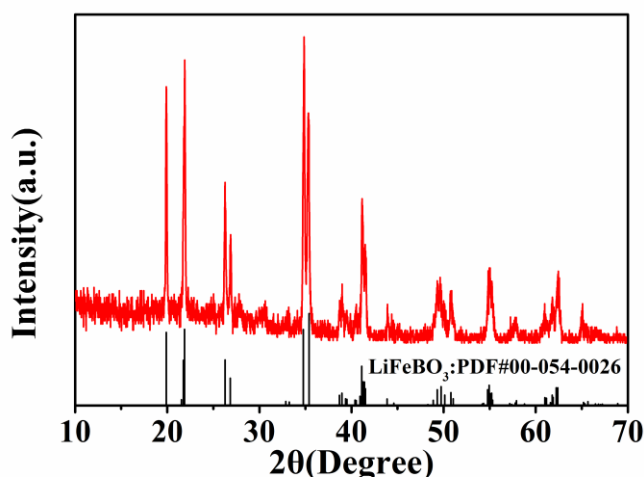
**Figure 1.** XRD of the $LiFeBO_3$ sample

The structure of the synthesized $LiFeBO_3$/C sample was determined by using the powder X-ray diffraction, as shown in Fig. 1. The diffraction peaks of the sample could be regarded as monoclinic $LiFeBO_3$ with a space group of C2/c, and no other peak is observed. The sharp diffraction peaks

indicate the excellent crystallinity of LiFeBO$_3$/C. No evidence of diffraction peaks for the carbon coating appears in the diffraction pattern of the sample, since carbon has an amorphous structure. The amount of carbon in LiFeBO$_3$/C is approximately 3.01wt%, as determined by the C S analysis method.

The morphology of the 3%GN+SP electrode was shown in Fig. 2. As shown in Fig. 2(a), spherical LiFeBO$_3$/C particles, which have a size distribution from 1 μm to 5 μm, are completely encased in conductive additives. Fig. 2(b) shows a magnified image of the 3%GN+SP electrode. The layered graphene is well mixed with Super P and uniformly spread over the LiFeBO$_3$/C electrode.
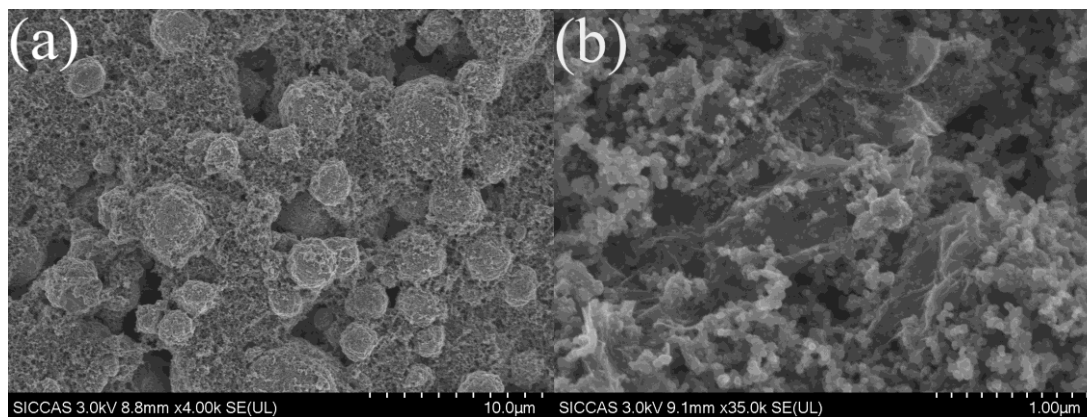
Figure 2. SEM images of the 3%GN+SP electrode at low (a) and high (b) magnification

The electrical conductivity tests were carried out by RTS-4 linear four-point probe system and the results are shown in Table 1. As the content of graphene increases, the electronic conductivity of the LiFeBO$_3$/C electrodes gradually increase. The electronic conductivity of the 3%GN+SP electrode is 9.63×10^{-3} S/cm, which is close to 2 times of that of the SP electrode (5.16×10^{-3} S/cm). When the graphene amount reaches 5%, the electronic conductivity attains 1.65×10^{-2} S/cm. The electronic conductivity improvement could be attributed to the 'plane-to-point' conduction mode and the liberated-π-electrons of the flaky graphene [22].

**Table 1**. The electronic conductivity of LiFeBO$_3$ / C electrodes with different amounts of graphene

Electrode	SP	1%GN+SP	3%GN+SP	5%GN+SP
Electronic Conductivity (S/cm)	5.16×10^{-3}	8.12×10^{-3}	9.63×10^{-3}	1.65×10^{-2}

Fig. 3 shows the typical charge/discharge curves of the LiFeBO$_3$/C electrodes with different amounts of graphene. The SP electrode delivers an initial discharge specific capacity of 174.5 mAh/g at 0.1 C. When the graphene is 1%, the initial discharge specific capacity of the 1%GN+SP electrode is 180.2 mAh/g. When the graphene content increases to 3%, the 3%GN+SP electrode exhibits the highest specific discharge capacity 189.6 mAh/g at 0.1 C. This high capacity may be mainly attributed to the electronic conductivity improvement of the LiFeBO$_3$/C electrodes by the graphene additive.

However, the enhancement in the discharge capacity cannot be maintained, when the graphene content is further increased. The specific discharge capacity of the 5%GN+SP electrode drops to 172.5 mAh/g. This decrease may result from excess graphene that might form a continuous phase hindering the diffusion of the electrolyte as well as Li^+.
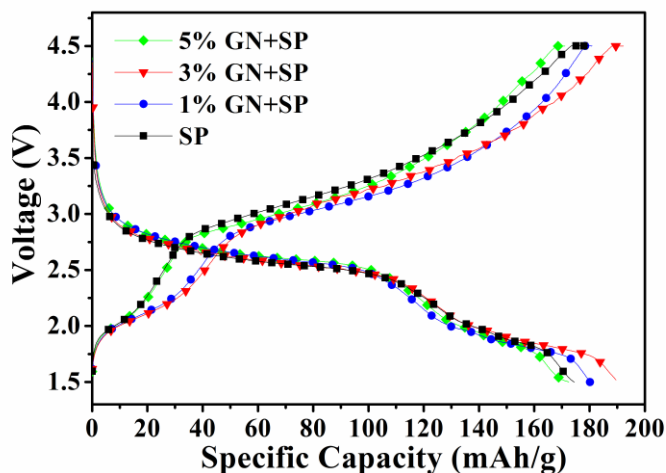
Figure 3. Initial charged-discharged performance of the $LiFeBO_3$/C electrodes with different amounts of graphene.
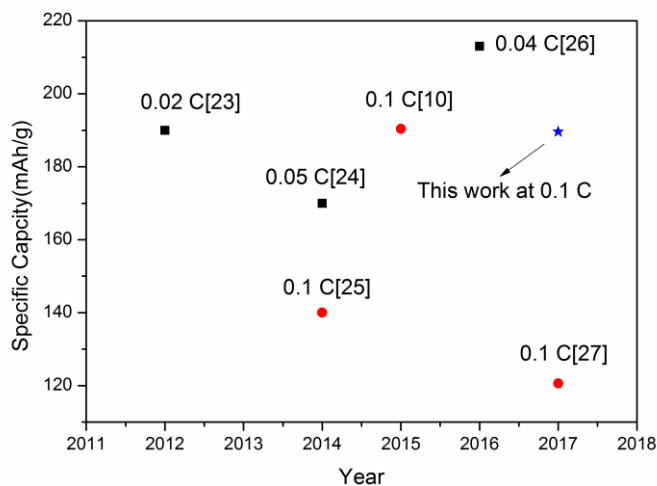

Figure 4. Comparison of the initial discharge capacities of $LiFeBO_3$/C obtained from references [10, 23-27] and this work.

Fig. 4 shows the main research progress of $LiFeBO_3$/C in recent years. As shown in Fig. 4, the initial discharge capacity of the 3%GN+SP electrode is 189.6 mAh g^{-1} at 0.1 C, which is better than most of the other $LiFeBO_3$/C samples reported [23-25, 27]. Bo reported that $LiFeBO_3$/C delivered an initial discharge capacity of 190 mAh g^{-1} at 0.02 C, which was obtained at a much lower rate [23]. Mesoporous $LiFeBO_3$/C hollow spheres, synthesized by Chen [10], exhibited a discharge capacity of 190mAh g^{-1} at 0.1 C, which is almost the same as in this work. Mesoporous $LiFeBO_3$/C, synthesized by Pechini Sol-gel method, had an initial discharge capacity of 213mAh g^{-1} at 0.04 C [26], which is

close to the theoretical value. However, the material's discharge capacity at 0.1 C had not been mentioned.

Fig. 5 shows the cycle and rate performance of the LiFeBO$_3$/C electrodes with different quantities of graphene in the voltage range from 1.5-4.5 V. As shown in Fig. 5(a), the SP electrode has a capacity retention of 89.0% after 50 cycles at 1 C. At first, the capacity retention rises with an increasing content of graphene conductive additives. The capacity retentions of the 1%GN+SP, 3%GN+SP electrodes are 94.6% and 95.1%, respectively. These retentions result from the electronic conductivity enhancement of the LiFeBO$_3$/C electrodes caused by graphene. However, the capacity retention of the 5%GN+SP electrode falls back to 92.5%. The discharge capacities of the LiFeBO$_3$/C electrodes with different amounts of graphene at various rates ranging from 0.1 C to 5 C are shown in Fig. 5(b). Among all the electrodes, the 3%GN+SP electrode has the highest specific discharge capacity at each rate. In addition, the superiority of the 3%GN+SP electrode declines with increasing discharge rate. The specific discharge capacity of the 3%GN+SP electrode is 189.6 mAh/g at 0.1 C, which is 15.1 mAh/g higher than that of the SP electrode. When the rate is as high as 5C, the discharge specific capacity of the 3%GN+SP electrode is 31.1 mAh g^{-1}, which is only 9.1 mAh g^{-1} higher than that of the SP electrode (22 mAh g^{-1}). The main factor restricting the specific discharge capacity is not only the electronic conductivity but also the ionic conductivity at high rates. Although the graphene could have improved the electronic conductivity of the LiFeBO$_3$/C electrodes, the ionic conductivity turns into the limiting step at high rates. The specific discharge capacity of the 5%GN+SP electrode is close to that of SP electrode from 0.1 C~1 C. However, its discharge specific capacity is obviously lower than that of SP electrode at a high rate (2 C and 5 C).
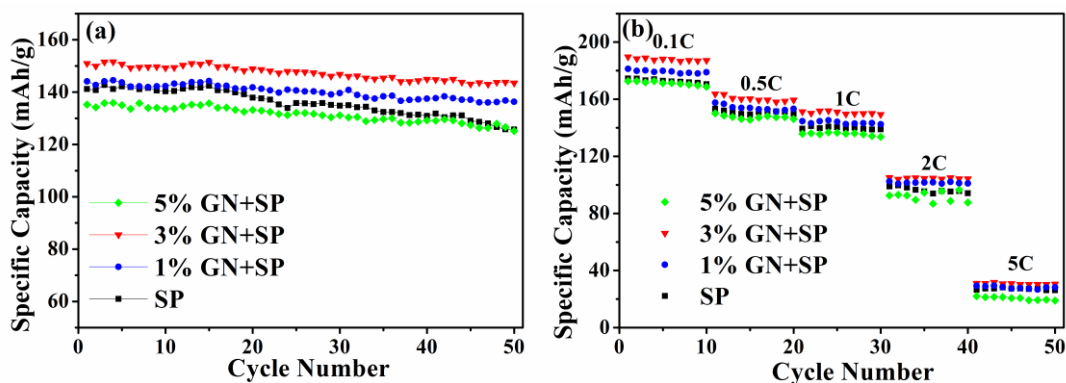
Figure 5. (a)Cycling performances of the LiFeBO$_3$/C electrodes with different amounts of graphene at 1 C, (b)Rate performance of the LiFeBO$_3$/C electrodes with different amounts of graphene at various rates from 0.1 C to 5 C

The results reveal that proper graphene conductive additives (~3%) could improve the rate performance of the LiFeBO$_3$/C electrodes, but if the content of graphene is more than 3%, then the local graphene may form a continuum, hindering the diffusion of Li$^+$, which limites its electrochemical performance. A similar phenomenon has been reported by Su [22], with the LiFePO$_4$ electrode using

graphene as a conductive additive. The flexible and super-thin graphene sheets are more easily form a conducting network with a low percolation threshold than the spherical SP particles.
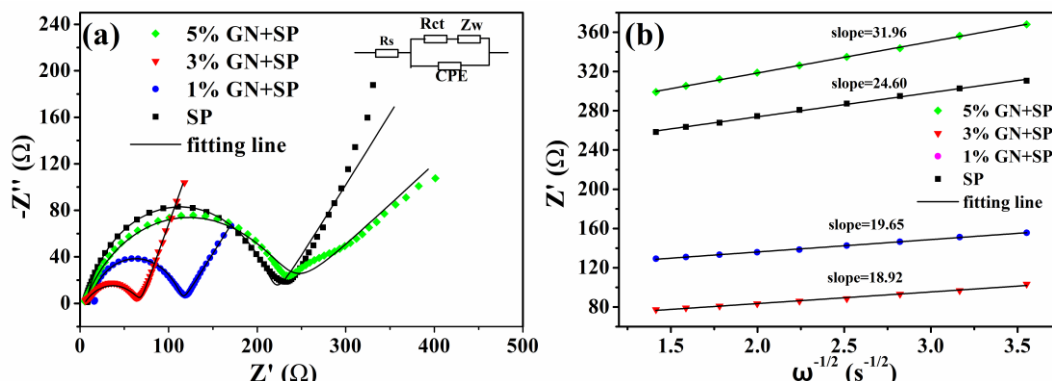
Figure 6. (a)The EIS plots of the LiFeBO$_3$/C electrodes with different amounts of graphene; and (b) the relationship between Z' and $\omega^{-1/2}$ at low frequencies

Table 2. Electrode kinetic parameters obtained from the equivalent circuit fitting of the LiFeBO$_3$/C electrodes with different amounts of graphene

Electrode	Rs (Ω)	Rct (Ω)	D_{Li} (cm^2 s^{-1})
SP	6.65	215	5.94×10^{-14}
1%GN+SP	5.28	105	9.13×10^{-14}
3%GN+SP	5.07	64.1	9.85×10^{-14}
5%GN+SP	6.31	220	3.45×10^{-14}

To verify the speculation, EIS testing was conducted. Before the EIS tests, several preliminary galvanostatic cycles were executed for stable SEI film formation and the good pervasion of the electrolyte into the active material. Fig. 6(a) demonstrates the Nyquist and fitting plots of the LiFeBO$_3$/C electrodes with different amounts of graphene after 10 cycles at 0.1 C, as well as the equivalent circuits. The Nyquist plots are composed of a semicircle in the high-frequency range and a line in the low-frequency range. The intercept on the Z´ axis in the high frequency part corresponds to the ohmic resistance (Rs) of the electrolyte. The semicircle in the high-to-medium frequency range is associated with the charge transfer resistance (Rct) on the interface of the electrolyte/electrode. The simulation parameters of the equivalent circuit, analyzed by the electrochemical workstation (Autolab PGSTAT302N), are listed in Table. 2. The Rct of the SP electrode is 215 Ω. The charge-transfer resistance (Rct) values of the 1%GN+SP and 3%GN+SP electrodes are 105 Ω and 64.1 Ω, respectively, which are both much smaller than that of the SP electrode. However, the charge-transfer resistance (Rct) increases with a further increase the content of graphene. The charge-transfer resistance (Rct) of the 5%GN+SP electrode increases to 220 Ω. The Rct is an important kinetics parameter of an electrochemical reaction, which influenced by many factors including the diffusion of ions, the conduction of electrons, temperature, etc. and so on [28,29]. The lithium ion diffusion coefficient (D$_{Li}$) can be calculated from formula (1)

$$D = R^2 T^2 / 2 A^2 n^4 F^4 C^2 \sigma^2 \qquad (1)$$

where R is the gas constant, T is the absolute temperature, n is the number of electrons transferred in the half-reaction for the redox couple, F is the Faraday constant, C is the concentration of lithium ions that can be calculated from formula (2) and σ is the slope of the line $Z' \sim \omega^{-1/2}$, as show in Fig. 5(b)

$$C = n/V = m/MV = \rho/M \qquad (2)$$

where F and R are constants with values of 96500 C mol^{-1} and 8.314 J K^{-1}mol^{-1}, respectively. A is the area of electrode, 1.13×10^{-4} m^2. T is 298 K, and n is 1. C is the ratio of the density and the molecular weight of the materials, which is 2.8×10^4 mol m^{-3}. The calculated D_{Li} of the SP electrode is 5.94×10^{-14} cm^2 s^{-1}. D_{Li} increases to 9.13×10^{-14} cm^2 s^{-1} for the 1%GN+SP electrode. When the amount of graphene conductive additives is 3%, its D_{Li} attains the largest value of 9.85×10^{-14} cm^2 s^{-1}. Shi [30] and Shin [15] also reported that both the electronic conductivity and ion diffusion coefficient of the LiFePO$_4$ electrodes could be increased by graphene. However, the Li ion diffusion coefficient of the 5%GN+SP electrode decreases to 3.45×10^{-14} cm^{2}s^{-1}. According to Su's work [22], excess graphene will agglomerate and hinder Li$^+$ diffusion. This result is consistent with the above speculation and proves that the proper amount of graphene conductive additives (~3%) could significantly improve both the electronic and ionic conductivity of the LiFeBO$_3$/C electrode. This improvement leads to the lowest Rct of the 3%GN+SP electrode. When the content of graphene exceeds 3%, the local graphene may form a continuum, hindering the diffusion of electrolyte, which leads to a decrease in the Li ion diffusion coefficient. Thus, the Rct of the 5%GN+SP electrode becomes the highest one.

4. CONCLUSIONS

The role of graphene as a conductive additive in the LiFeBO$_3$/C electrode is investigated. The 3%GN+SP electrode shows the highest capacity of 189.6 mAh/g at 0.1 C, which is 15.1 mAh/g higher than that of the SP electrode. The cyclic retention of the 3%GN+SP electrode is 95.1% after 50 cycles at 1 C, which is much better than that of the SP electrode (89%). The graphene conductive additive to some extent improves the rate performance of the LiFeBO$_3$/C electrodes. The discharge capacity of the 3%GN+SP electrode is 31.1 mAh/g at 5 C, which is 1.4 times higher than that of the SP electrode (22 mAh/g). The electronic conductivity of the LiFeBO$_3$/C electrodes increases with an increase in graphene. The lithium ion diffusion coefficient increases initially, then sharply decreases when the graphene content reaches 5%. These results can be attributed to the fact that a proper amount of graphene conductive additive can improve both the electronic conductivity and ionic diffusion coefficient of the LiFeBO$_3$/C electrode, thus increasing its electrochemical performance.

References

1   Z.A. Zhang, Z.Y. Zhang, W. Chen, G.C. Wang, J Liu and Y.Q. Lai, *New J. Chem.*, 39 (2015) 3765.
2   F. Yu, J.J. Zhang, Y.F. Yang and G.Z. Song, *J. Power Sources*, 195 (2010) 6873.
3   X.H. Tian, Y.K. Zhou, X.F. Tu, Z.T. Zhang and G.D. Du., *J. Power Sources*, 340 (2017) 40.
4   V. Legagneur, Y. An, A. Mosbah, R. Portal, A. Le Gal La Salle, A. Verbaere, D. Guyomard and Y. Piffard, *Solid State Ionics*, 139 (2001) 37.
5   A.P. Tang, D.H. He, Z.Q. He, G.R. Xu, H.S. Song and R.H. Peng, *J. Power Sources*, 275 (2015) 888.
6   B. Zhang, L. Ming, J.C. Zheng, J.F. Zhang, C. Shen, Y.D. Han, J.L. Wang and S.E. Qin, *J. Power Sources*, 261 (2014) 249.
7   Y.Z. Dong, Y.M. Zhao and Z.D. Shi, *Electrochim. Acta*, 53 (2008) 2339.
8   Y.Z. Dong, Y.M. Zhao and P.J. Fu, *J. Alloys and Compounds*, 461 (2008) 585.
9   A. Yamada, N. Iwane, Y. Harada, S.I. Nishimura, Y. Koyama and I. Tanaka, *Adv. Mater.*, 22 (2010) 3583.
10 Z.X Chen, L.F Cao, L. Chen, H.H. Zhou, C.M. Zheng, K. Xie and Y.F. Kuang, *J. Power Sources*, 298 (2015) 355.
11 J.C. Zheng, S.E. Qin, B. Zhang, X. Ou, L. Ming and C. Shen, *Chem. Lett.*, 43 (2014) 1411.
12 A. Yamada, N. Iwane, S.I. Nishimura, Y.Koyama and I. Tanaka, *J. Mater. Chem.*, 22 (2011) 10690.
13 Z.P. Li, Y.P. Wang,Q.R. Hu, Y. Yang, Z.C. Wu and C.M. Ban, *J. Nanosci. Nanotechnol.*, 15 (2015) 7186.
14 M.A. Cambaz, M.A. Reddy, B.P.Vinayan and R. Witte, *ACS Appl. Mater. Interfaces*, 8 (2016) 2166.
15 H.C. Shin, W.I. Cho and H. Jang, *Electrochim. Acta*, 52 (2006) 1472.
16 Y. Liu, X. Li, H. Guo, Z.X. Wang, W.J. Peng, Y. Yang and R.F. Liang, *J. Power Sources*, 184 (2008) 522.
17 L. Ke, W. Lv, F.Y. Su, Y.B. He, C.H. You, B.H. Li, Z.J. Li, Q.H. Yang and F.Y. Kang, *Carbon*, 92 (2015) 311.
18 T. Liu, S.M. Sun, Z. Zang, X.C. Li, X.L. Sun, F.T. Cao and J.F. Wu, RSC Adv., 7 (2017) 20882.
19 F.Y. Su, C. You, Y.B. He, W. Lv, W. Cui, F.M. Jin, B.H. Li, Q.H. Yang and F.Y. Kang, *J. Mater. Chem.,* 20 (2010) 9644.
20 W.J. Ren, K. Wang, J.L. Yang, R. Tan, J.T. Hu, H. Guo, Y.D. Duan, J.X. Zheng, Y. Lin and F. Pan, *J. Power Sources*, 331 (2015) 232.
21 C. Gong, Z. Xue, S. Wen, Y. Ye and X. Xie, *J. Power Sources*, 318 (2016) 93–112.
22 F.Y. Su, C.H. You, Y.B. He, W. Lv, W. Cui, F.M. Jin, B.H. Li, Q.H. Yang and F.Y. Kang, *J. Mater. Chem.*, 20 (2010) 9644
23 S.H. Bo, F. Wang, Y. Janssen, D.L. Zeng, K. Nam, W.Q. Xu, L.S. Du, J. Graetz, X.Q. Yang, Y.M. Zhu, J.B. Parise, C.P. Grey and P.G. Khalifah, *J. Mater. Chem.*, 22 (2012) 8799.
24 L. Tao, G. Rousse, J.N. Chotard, L. Dupont, S. Bruy`ere, D. Hanˇzel, G. Mali, R. Dominko, S. Levasseur and C. Masquelier, *J. Mater. Chem. A*, 2 (2014) 2060.
25 B. Zhang, L. Ming, J.C. Zheng, J.F. Zhang, C. Shen, Y.D. Han, J.L. Wang and S.E. Qin,*J. Power Sources*, 261 (2014) 249.
26 G. Sánchez, V.T. Gonzalez, L. Sanchez, E. Garza and Lorena, *Dig J Nanomater Bios*, 11 (2016) 1063.

27 X.F. Gu, M. Ting and S Zhi, *J Sol-Gel Sci Technol,* 81 (2017) 362.
28 L. Liao, P. Zuo, Y. Ma, X. Chen, Y. An, Y. Gao and G. Yin, *Electrochim. Acta*, 60 (2012) 269.
29 X.X. Dong, C.Y. Huang, Q. Jin, J. Zhou, P. Feng, F.Y. Shi and D.Y. Zhang, *RSC Adv*., 7 (2017) 33745
30 Y. Shi, S.L. Chou, J.Z. Wang, D. Wexler, H.J. Li, H.K. Liu and Y.P. Wu, *J. Mater. Chem.*, 22 (2012) 16465